

Design of a visible dual broadband nearly perfect absorber

XIULI JIA

School of Mathematics and Physics, Bohai University,
Liaoning, Jinzhou 121013, China; jiaxiuli_hit@163.com

Many optical systems benefit from elements that can absorb a broad range of wavelengths over a wide range of angles, independent of polarization. In this paper, we present a nearly perfect absorber with dual broadband and polarization-independent in the visible regime that exploits strong symmetric and asymmetric resonance modes of electromagnetic dipoles. It makes use of a bilayer hollowed-out cross pattern structure which is simple, having five layers that include two stacks of metal film with hollowed-out ribbon in cross patterns, two dielectric spacers, and a metal reflecting layer. Simulations show that the design exhibits a significantly enhanced absorption property when compared to a device with a normal cross pattern structure. The nearly perfect absorption efficiency of the device is above 98.5% at two resonances regimes: from 5.57×10^{14} to 6.08×10^{14} Hz and from 6.75×10^{14} to 7.05×10^{14} Hz, and its stable absorption characteristics can be maintained over a wide range of polarizing angle – up to $\pm 90^\circ$. This strategy can, in principle, be applied to other material systems and could be useful in diverse applications, including thermal emitters, photovoltaics, and photodetectors.

Keywords: metamaterials, visible absorber, polarization-independent, nearly perfect absorption.

1. Introduction

The energy of light is regarded as one of the most abundant yet least harvested, sources of renewable energy. Metamaterials that are characterized by their unique perfect or nearly perfect absorption properties have attracted substantial attention along with their development in many applied fields such as color filters [1, 2], photodetectors [3, 4], photovoltaics [5–7] sensors [8, 9], bolometers [10], optical lithography [11], and thermal emitters [12, 13]. Much more effort will be devoted in the future to developing highly efficient light absorption.

The prior literature describes the extensive efforts that have been devoted to various absorption structures such as nanodisks, nanowires, nanocones, and arrays of nano-holes; and the working frequency bands of these nanostructures have steadily moved to higher frequencies while retaining unique optical and electric characteristics for light absorption [14–24]. However, the earlier versions of absorption structures had

relatively narrow bandwidths; recently, more attention has shifted to saw-toothed metamaterials made by stack structure of multilayer materials that exhibit extraordinary electromagnetic properties, and had wilder absorption bands with higher absorption [25, 26] – particularly the polarization independent metamaterial absorbers and their thermo-photovoltaic applications [27, 28]. The spectrum selective absorption of metamaterials is based on the resonance mechanism of nanostructures, where the absorption bandwidth and intensity can be engineered by controlling the size and geometry of the nanostructures, and different resonance modes result in different absorption mechanisms. Not only do metamaterials promise unprecedented flexibility in controlling the flow of light in sometimes counterintuitive ways, they suggest new opportunities to incorporate electrical and optical functions in a unified platform [29]. This is because the metallic nanostructures that provide engineered plasmonic behavior for the metamaterial can also fulfill the conventional roles of metals for voltage bias, carrier injection, and current extraction. The plasmonic absorbers using phase-change metamaterial have been most extensively studied in visible and mid-infrared [30–34]. Moreover, CUI *et al.* recently reported a 1D metamaterial based sawtooth-shaped absorber that shows good absorption in the middle infrared waveband [25]. LIANG *et al.* developed a 2D pyramidal-shaped metamaterial absorber that shows surprisingly high absorption over an extraordinarily broad waveband ranging from the near infrared to long infrared [26]. Both of these studies are focused on absorption in the infrared waveband mainly. The absorption bandwidth is broad but the geometric structure is complex. Different treatment methods have been used to deal with different absorption characteristics in multilayer architectures [35], metamaterials [36–38], and nanostructures with subwavelength gratings [39].

The visible band from 3.8×10^{14} to 7.8×10^{14} Hz accounts for nearly half of the total energy in the solar spectrum; thus, the development of an absorber that functions well in the visible band is necessary. Here, we propose an efficient absorption structure based on strong symmetric and asymmetric resonance modes of electromagnetic dipoles; we employ numerical simulation to determine its wide-polarizing angle absorption properties, its sensitivity to the polarization state of the incident light, and its bandwidth. Two stacks of hollow-out cross sheet-metal provide the resonance mechanism for absorption, and a metal functional layer can prevent light transmission effectively. Additionally, the performance of our device is almost independent of the angle of incidence from 30° to 90° as well as the incident light. We believe that such a design will enhance the functionality of metamaterial absorbers and should be valuable in many applications such as sensors, solar cells, and metamaterials in general.

2. Dual broadband, polarization-independent, and nearly perfect absorption design

Figure 1 illustrates the geometry and important properties of the structure. Silicon dioxide and silver were chosen for their desirable optical properties over the frequency range of interest. The bilayer silver (Ag) nano hollowed-out cross (HC) patterns structure

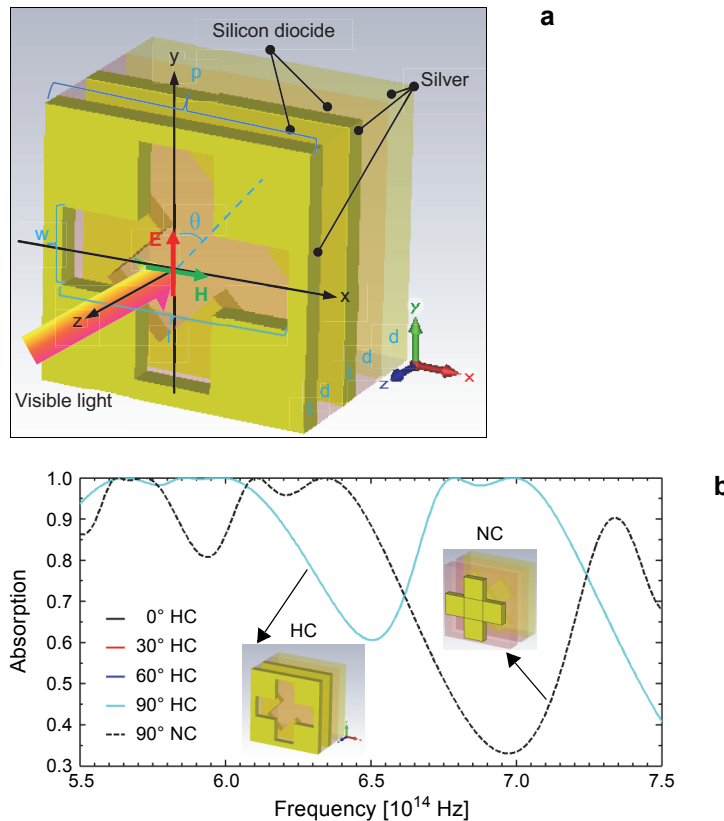


Fig. 1. Schematic diagram of the proposed polarization-independent, wide-angle and broadband visible absorber with improved viewing angle employing electromagnetic dipoles resonance behaviors in highly absorbing metamaterials (a). Simulated absorption spectrum obtained from bilayer HC pattern structure and bilayer NC pattern structure configurations under different polarization light incident (b).

(Fig. 1a) provide both symmetric and antisymmetric resonances, along with the angle -sensitive, polarization insensitive broadband absorption properties. The device structure simply consists of a Ag functional layer on the bottom, followed by a SiO₂ layer, the third layer of Ag nano HC pattern with angular offsets of 45° from the x-axis, then another SiO₂ layer, and the last layer of Ag nano HC pattern with angular offsets of $\theta = 45^\circ$ with respect to the previous Ag nano HC pattern layer. The length l and width w of the Ag nano HC pattern are 300 and 100 nm, respectively. The thickness t of Ag nano cross patterns, SiO₂ layer and Ag functional layer are 33, 70, and 70 nm, respectively. The unit size p is 350 nm. With these optimized geometric parameters it is possible to achieve dual-band and broadband absorption characteristic with nearly perfect absorption efficiency in the visible range, as shown in Fig. 1b. It is obvious that the absorption spectrum is greatly broadened by introducing an additional resonance for HC stacks as compared to the normal cross (NC) pattern structure. SiO₂ material is utilized in semiconductor devices, the forbidden bandwidth variability of SiO₂ can be

exploited for its use as a light absorption layer in thin film amorphous silicon solar cells to improve the efficiency of broadband light absorption [40, 41], and Ag functions as a reflective mirror since it is highly reflective and has the lowest absorption loss among noble metals. The overall absorption could be even enhanced by employing loss metals such as aluminum (Al), copper (Cu), and chromium (Cr), which are often used in the microwave band. However, for high-frequency bands such as visible light, they can be affected by metal skin effect. So Al or Ag is used in high-frequency bands, and we chose Ag in this visible absorber. We aim at designing the structure with the improved absorption property only in the cross pattern layers, thus potentially extending the range of possible applications, including tandem PV systems. In our absorber design, the thickness of a top metallic film is designed to be optically transparent (33 nm) so that it allows incident light to pass through a middle dielectric layer to create an additional resonance at different wavelength, thereby making the bandwidth broad, whereas a bottom metallic function layer is 70 nm that is thick enough to prevent any transmitted light, thus validating the equation $A = 1 - R$, where A is the total absorption and R is the reflection.

This HC pattern structure has multiple effects which include the extraordinary optical transmission (EOT) and chirality. The overall structure of the three layers of metal is mingled with dielectric layers in which two layers of metal of the HC pattern are thin enough (33 nm, less than the skin depth of the incident wave) and can let the incident light through. At the same time, the design of the hollowed-out can increase the EOT effect. The bottom and top layer of HC pattern has a certain angle to produce chiral. The bottom of the metal function layer is thick enough (70 nm) to prevent light from passing through.

First, a simulated absorption spectrum of the proposed HC structure device (blue solid line) is described along with that of the NC structure (black dashed line) for the comparison in Fig. 1b. As can be seen from the figure, our proposed HC structure exhibits two broader nearly perfect absorption bands: from 5.57×10^{14} to 6.08×10^{14} Hz and from 6.75×10^{14} to 7.05×10^{14} Hz performance of 98.5%, which arises from four distinctive resonances regimes appearing at around 5.57×10^{14} , 6.08×10^{14} , 6.75×10^{14} , and 7.05×10^{14} Hz, while the NC structure also shows four resonances 5.25×10^{14} , 5.64×10^{14} , 6.11×10^{14} , and 6.35×10^{14} Hz. At 0° to 90° polarizations incidence of linearly polarized beam, the absorption of HC remains constant, which proves that the structure has the polarization independent characteristics for linearly polarized light from 5.5×10^{14} to 7.5×10^{14} Hz.

The cross pattern metamaterial is essentially an electric ring resonator (ERR), and evolved from metallic cut-wire. YE *et al.* studied the metallic cut-wire structure proceed system [42]. In the metallic cut-wire, electric dipole resonance can be produced at both ends of wire and have opposite polarity. Electric dipole resonance produced oscillation in contrast to the metal surface, to at the same time equivalent magnetic dipole, with the strong magnetic field response by magnetic dipole resonance resulting electromagnetic wave absorption effect. But single metallic cut-wire absorber is more sensitive to the polarization direction of incident wave, in addition to missing magnetic compo-

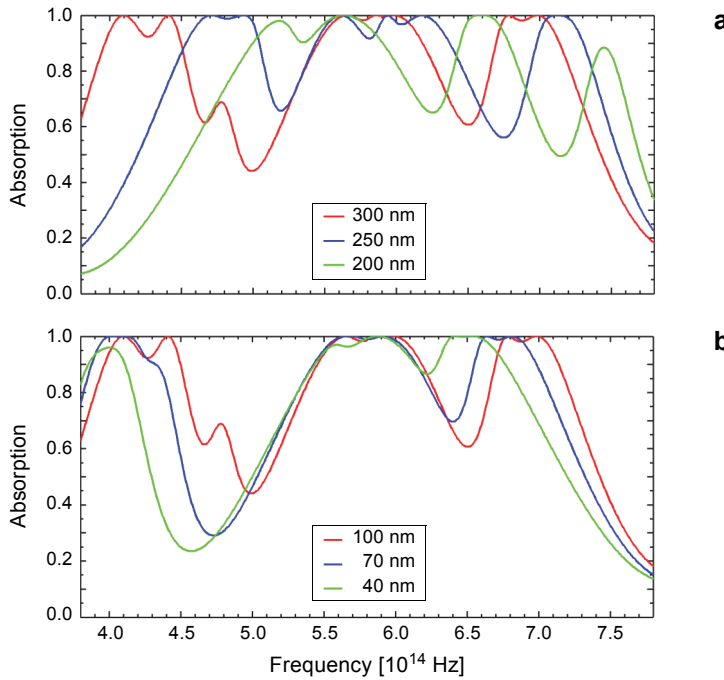


Fig. 2. Simulated geometric parameters of hollow-out cross pattern resolved absorption spectrum for HC structure: length (a) and width (b).

ment for the plane wave incidence in the tangent direction to it. On the contrary, the orthogonal cross structure is insensitive to the angle and to polarization direction incidence for both have the x and y component. Based on a similar resonant frequency of the bilayer orthogonal cross structure, the absorption bandwidth can be extended.

Next, we examine the dependence of the absorption efficiency on the length and width change in the HC structure as shown in Fig. 2. In Figure 2a, the calculated curves of the optical absorption as a function of the length of HC structure and the frequency are shown, given fixed thickness of the sheet-metal and dielectric layers. The absorption spectrum shifts to the higher frequency when we reduce the length of HC structure, and the absorption bandwidth is narrowed. In addition, the number of perfect absorption peaks is gradually reduced, from six resonance perfect absorption peaks reduced to two, that is because metal loss increases under the influence of the skin effect of metal by reducing its size. In Fig. 2b, the calculated curves of the optical absorption as a function of the width of structure and the frequency are shown, given fixed thickness of the sheet-metal and dielectric layers. The absorption spectrum shifts to the lower frequency when we reduce the hollow-out width of HC structure, and the absorption bandwidth is narrowed. In addition, the number of perfect absorption peaks is also reduced, from six resonance perfect absorption peaks to two.

The magnetic dipole resonance absorption frequency of the cross structure is mainly caused by the length of the tangent, so the absorption bandwidth can be extended

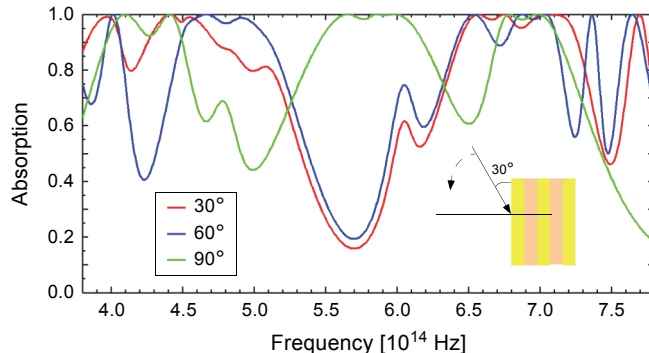


Fig. 3. Simulated absorption spectrum obtained from different incident angles: 30°, 60° and 90°.

by superposition of different resonant frequencies. Different tangent lengths of bilayer orthogonal cross structure increased the difficulty of the metamaterial preparation. By adjusting the thickness of the dielectric layer between each orthogonal cross layer, the free space impedance matching of each orthogonal cross layer can be achieved, respectively. The thickness of the dielectric for each metal layer decides about the electric dipole resonance strength and the magnetic resonance strength of the functional layer. So by adjusting the thickness of the dielectric layer one can also modulate the impedance, in order to achieve the free space impedance matching, and to achieve maximum absorption efficiency purpose [43].

More detailed investigations on what is the influence on the absorption of the incident angle are presented in Fig. 3. Figure 3 shows simulated absorption spectra of the proposed HC structure at 30° to 90° incidence, where the absorption A is obtained from equation $A = 1 - R$. As is seen from the figures, the broadbands 100% of perfect absorptions are achieved at the resonance absorption peak regimes, respectively from the simulation. When linear polarized lights incidence is with 30°, 60° and 90°, the absorption band moves to the low frequency direction with the increase of the incident angle as shown in Fig. 3. However, the absorption bandwidth increased with the increase in the incident angle. Thus, a high absorption band above 92.5% is from 3.98×10^{14} to 4.50×10^{14} Hz and two nearly perfect absorption bands above 98.5% at resonance regimes from 5.57×10^{14} to 6.08×10^{14} Hz, and from 6.75×10^{14} to 7.05×10^{14} Hz are obtained by linearly polarized light incident perpendicularly.

3. Physical mechanism of the absorption

In order to understand the mechanism of the resonances for the HC structure design, we studied the surface current distributions as shown in Fig. 4. Here we take 5.65×10^{14} Hz as an example. In hollow-out space of the first layer of sheet-metal, where the current distribution directions of the upper and the lower surface are antiparallel and forms an asymmetric resonance mode. In non-hollow space of the first layer of sheet-metal,

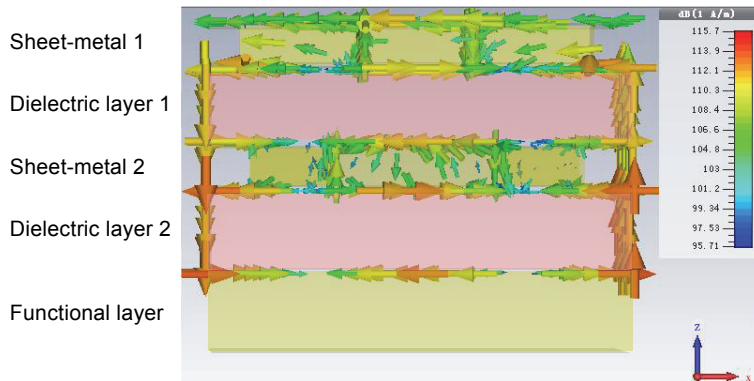


Fig. 4. The simulated surface current distribution for HC structure at perfect absorption resonance frequency 5.65×10^{14} Hz. The cones in red show the direction and magnitude of the surface current. The magnitude of the surface current is also shown by the color on the wires, with red and blue corresponding to largest and smallest values.

where the current distribution directions are parallel and forms a symmetric resonance mode. At the second layer of sheet-metal, the current distribution directions of the upper and lower surface are antiparallel both in hollow-out space and out of it. In the first, the second, and the functional sheet-metal layers, the current direction in the interfaces of the sheet-metal are opposite. The current distribution shows that the cross pattern pairs can be viewed as a chiral version of the short wire pairs [44], which has similar current distributions in the symmetric and asymmetric resonance modes.

This HC pattern structure has multiple effects which include the extraordinary optical transmission (EOT) and chirality [43]. Compared with NC pattern structure, the hollow structure can enhance the coupling between units and achieve greater magnetic losses. But beyond that, in the light-matter interaction, the incident light transforms into evanescent wave. Based on the above two points, the hollow structure achieves a wider absorption band [45, 46].

4. Conclusion

In summary, we have demonstrated bilayer HC pattern structure with very adaptable properties, and we have demonstrated a polarization-independent, dual broadband, and nearly perfect absorption in the visible range utilizing the symmetric and asymmetric resonance mode effects in the HC structure. In contrast to the first nearly perfect absorption band of NC pattern structure, the HC structure's first nearly perfect absorption band is more than two times as broad. This intersection angle introduces symmetric and asymmetric resonance modes of electromagnetic dipoles and the perfect absorption peaks are achieved at different resonances. The geometry of HC design is simple and easy to fabricate, and is therefore more suitable for optical frequency applications than other types of metamaterial designs. These features are highly desired for various

applications such as photovoltaics, thermal emitters, photodetectors, and metamaterials in general.

Acknowledgments – The author acknowledges the support by the Doctoral Startup Fund of Bohai University (No. 0517bs027), the National Natural Science Foundation of China (No. 11847007) and the Liaoning Provincial Natural Science Foundation of China (No. 20180540035).

References

- [1] XU T., WU Y.-K., LUO X., GUO L.J., *Plasmonic nanoresonators for high-resolution colour filtering and spectral imaging*, Nature Communications **1**, 2010, article ID 59, DOI: [10.1038/ncomms1058](https://doi.org/10.1038/ncomms1058).
- [2] WU Y.-K.R., HOLLOWELL A.E., ZHANG C., GUO L.J., *Angle-insensitive structural colours based on metallic nanocavities and coloured pixels beyond the diffraction limit*, Scientific Reports **3**, 2013, article ID 1194, DOI: [10.1038/srep01194](https://doi.org/10.1038/srep01194).
- [3] ROSENBERG J., SHENOI R.V., VANDERVELDE T.E., KRISHNA S., PAINTER O., *A multispectral and polarization-selective surface-plasmon resonant midinfrared detector*, Applied Physics Letters **95**(16), 2009, article ID 161101, DOI: [10.1063/1.3244204](https://doi.org/10.1063/1.3244204).
- [4] YU Z., VERONIS G., FAN S., BRONGERSMA M.L., *Design of midinfrared photodetectors enhanced by surface plasmons on grating structures*, Applied Physics Letters **89**(15), 2006, article ID 151116, DOI: [10.1063/1.2360896](https://doi.org/10.1063/1.2360896).
- [5] PANOU N.C., OSGOOD R.M., *Enhanced optical absorption for photovoltaics via excitation of waveguide and plasmon-polariton modes*, Optics Letters **32**(19), 2007, pp. 2825–2827, DOI: [10.1364/OL.32.002825](https://doi.org/10.1364/OL.32.002825).
- [6] CATCHPOLE K.R., POLMAN A., *Plasmonic solar cells*, Optics Express **16**(26), 2008, pp. 21793–21800, DOI: [10.1364/OE.16.021793](https://doi.org/10.1364/OE.16.021793).
- [7] NAKAYAMA K., TANABE K., ATWATER H.A., *Plasmonic nanoparticle enhanced light absorption in GaAs solar cells*, Applied Physics Letters **93**(12), 2008, article ID 121904, DOI: [10.1063/1.2988288](https://doi.org/10.1063/1.2988288).
- [8] LIU N., MESCH M., WEISS T., HENTSCHEL M., GIessen H., *Infrared perfect absorber and its application as plasmonic sensor*, Nano Letters **10**(7), 2010, pp. 2342–2348, DOI: [10.1021/nl9041033](https://doi.org/10.1021/nl9041033).
- [9] TITTL A., MAI P., TAUBERT R., DREGELY D., LIU N., GIessen H., *Palladium-based plasmonic perfect absorber in the visible wavelength range and its application to hydrogen sensing*, Nano Letters **11**(10), 2011, pp. 4366–4369, DOI: [10.1021/nl202489g](https://doi.org/10.1021/nl202489g).
- [10] MAHJOURI-SAMANI M., ZHOU Y.S., HE X.N., XIONG W., HILGER P., LU Y.F., *Plasmonic-enhanced carbon nanotube infrared bolometers*, Nanotechnology **24**(3), 2013, article ID 035502, DOI: [10.1088/0957-4484/24/3/035502](https://doi.org/10.1088/0957-4484/24/3/035502).
- [11] HUO F., ZHENG G., LIAO X., GIAM L.R., CHAI J., CHEN X., SHIM W., MIRKIN C.A., *Beam pen lithography*, Nature Nanotechnology **5**(9), 2010, pp. 637–640, DOI: [10.1038/nnano.2010.161](https://doi.org/10.1038/nnano.2010.161).
- [12] DIEM M., KOSCHNY T., SOUKOULIS C.M., *Wide-angle perfect absorber/thermal emitter in the terahertz regime*, Physical Review B **79**(3), 2009, article ID 033101, DOI: [10.1103/PhysRevB.79.033101](https://doi.org/10.1103/PhysRevB.79.033101).
- [13] ABBAS M.N., CHENG C.W., CHANG Y.C., SHIH M.H., CHEN H.H., LEE S.C., *Angle and polarization independent narrow-band thermal emitter made of metallic disk on SiO₂*, Applied Physics Letters **98**(12), 2011, article ID 121116, DOI: [10.1063/1.3571442](https://doi.org/10.1063/1.3571442).
- [14] HE L., JIANG C., RUSLI, LAI D., WANG H., *Highly efficient Si-nanorods/organic hybrid core-sheath heterojunction solar cells*, Applied Physics Letters **99**(2), 2011, article ID 021104, DOI: [10.1063/1.3610461](https://doi.org/10.1063/1.3610461).
- [15] MUSKENS O., RIVAS J.G., ALGRA R.E., BAKKERS E.P.A., LAGENDIJK A., *Design of light scattering in nanowire materials for photovoltaic applications*, Nano Letters **8**(9), 2008, pp. 2638–2642, DOI: [10.1021/nl0808076](https://doi.org/10.1021/nl0808076).

- [16] LIN C., POVINELLI M.L., *Optical absorption enhancement in silicon nanowire arrays with a large lattice constant for photovoltaic applications*, Optics Express **17**(22), 2009, pp. 19371–19381, DOI: [10.1364/OE.17.019371](https://doi.org/10.1364/OE.17.019371).
- [17] FANG H., LI X., SONG S., XU Y., ZHU J., *Fabrication of slantingly-aligned silicon nanowire arrays for solar cell applications*, Nanotechnology **19**(25), 2008, article ID 255703, DOI: [10.1088/0957-4484/19/25/255703](https://doi.org/10.1088/0957-4484/19/25/255703).
- [18] KELZENBERG M.D., TURNER-EVANS D.B., KAYES B.M., FILIER M.A., PUTNAM M.C., LEWIS N.S., ATWATER H.A., *Photovoltaic measurements in single-nanowire silicon solar cells*, Nano Letters **8**(2), 2008, pp. 710–714, DOI: [10.1021/nl072622p](https://doi.org/10.1021/nl072622p).
- [19] STELZNER T., PIETSCH M., ANDRÄ G., FALK F., OSE E., CHRISTIANSEN S., *Silicon nanowire-based solar cells*, Nanotechnology **19**(29), 2008, article ID 295203, DOI: [10.1088/0957-4484/19/29/295203](https://doi.org/10.1088/0957-4484/19/29/295203).
- [20] HU L., CHEN G., *Analysis of optical absorption in silicon nanowire arrays for photovoltaic applications*, Nano Letters **7**(11), 2007, pp. 3249–3252, DOI: [10.1021/nl071018b](https://doi.org/10.1021/nl071018b).
- [21] ZHU J., YU Z., BURKHARD G.F., HSU C.M., CONNOR S.T., XU Y., WANG Q., McGEEHEE M., FAN S., CUI Y., *Optical absorption enhancement in amorphous silicon nanowire and nanocone arrays*, Nano Letters **9**(1), 2009, pp. 279–282, DOI: [10.1021/nl802886y](https://doi.org/10.1021/nl802886y).
- [22] LI J., YU H., WONG S.M., ZHANG G., SUN X., LO P.G.Q., KWONG D.L., *Si nanopillar array optimization on Si thin films for solar energy harvesting*, Applied Physics Letters **95**(3), 2009, article ID 033102, DOI: [10.1063/1.3186046](https://doi.org/10.1063/1.3186046).
- [23] HUANG Y.F., CHATTOPADHYAY S., JEN Y.J., PENG C.Y., LIU T.A., HSU Y.K., PAN C.L., LO H.C., HSU C.H., CHANG Y.H., LEE C.S., CHEN K.H., CHEN L.C., *Improved broadband and quasi-unidirectional anti-reflection properties with biomimetic silicon nanostructures*, Nature Nanotechnology **2**(12), 2007, pp. 770–774, DOI: [10.1038/nnano.2007.389](https://doi.org/10.1038/nnano.2007.389).
- [24] HAN S., CHEN G., *Optical absorption enhancement in silicon nanohole arrays for solar photovoltaics*, Nano Letters **10**(3), 2010, pp. 1012–1015, DOI: [10.1021/nl904187m](https://doi.org/10.1021/nl904187m).
- [25] CU Y., FUNG K.H., XU J., MA H., JIN Y., HE S., FANG N.X., *Ultrabroadband light absorption by a sawtooth anisotropic metamaterial slab*, Nano Letters **12**(3), 2012, pp. 1443–1447, DOI: [10.1021/nl204118h](https://doi.org/10.1021/nl204118h).
- [26] LIANG Q., WANG T., LU Z., SUN Q., FU Y., YU W., *Metamaterial-based two dimensional plasmonic subwavelength structures offer the broadest waveband light harvesting*, Advanced Optical Materials **1**(1), 2013, pp. 43–49, DOI: [10.1002/adom.201200009](https://doi.org/10.1002/adom.201200009).
- [27] AGARWAL S., PRAJAPATI Y.K., SINGH V., SAINI J.P., *Polarization independent broadband metamaterial absorber based on tapered helical structure*, Optics Communications **356**, 2015, pp. 565–570, DOI: [10.1016/j.optcom.2015.08.055](https://doi.org/10.1016/j.optcom.2015.08.055).
- [28] AGARWAL S., PRAJAPATI Y.K., *Analysis of metamaterial-based absorber for thermo-photovoltaic cell applications*, IET Optoelectronics **11**(5), 2017, pp. 208–212, DOI: [10.1049/iet-opt.2016.0169](https://doi.org/10.1049/iet-opt.2016.0169).
- [29] CAI W., SHALAEV V., *Optical Metamaterials: Fundamentals and Applications*, Springer, New York 2010, DOI: [10.1007/978-1-4419-1151-3](https://doi.org/10.1007/978-1-4419-1151-3).
- [30] DONG W., QIU Y., YANG J., SIMPSON R.E., CAO T., *Wideband absorbers in the visible with ultrathin plasmonic-phase change material nanogratings*, The Journal of Physical Chemistry C **120**(23), 2016, pp. 12713–12722, DOI: [10.1021/acs.jpcc.6b01080](https://doi.org/10.1021/acs.jpcc.6b01080).
- [31] CAO T., WEI C.W., SIMPSON R.E., ZHANG L., CRYAN M.J., *Broadband polarization-independent perfect absorber using a phase-change metamaterial at visible frequencies*, Scientific Reports **4**(2), 2014, article ID 3955, DOI: [10.1038/srep03955](https://doi.org/10.1038/srep03955).
- [32] CAO T., ZHANG L., SIMPSON R.E., CRYAN M.J., *Mid-infrared tunable polarization-independent perfect absorber using a phase-change metamaterial*, Journal of the Optical Society of America B **30**(6), 2013, pp. 1580–1585, DOI: [10.1364/JOSAB.30.001580](https://doi.org/10.1364/JOSAB.30.001580).
- [33] CAO T., WANG S., WEI C.W., *Simulation of tunable metamaterial perfect absorber by modulating Bi₂Se₃ dielectric function*, Materials Express **6**(1), 2016, pp. 45–52, DOI: [10.1166/mex.2016.1277](https://doi.org/10.1166/mex.2016.1277).

- [34] CAO T., WEI C., SIMPSON R.E., ZHANG L., CRYAN M.J., *Rapid phase transition of a phase-change metamaterial perfect absorber*, Optical Materials Express **3**(8), 2013, pp. 1101–1110, DOI: [10.1364/OME.3.001101](https://doi.org/10.1364/OME.3.001101).
- [35] ULRICH C., PETERS M., BLÄSI B., KIRCHARTZ T., GERBER A., RAU U., *Enhanced light trapping in thin-film solar cells by a directionally selective filter*, Optics Express **18**(S2), 2010, pp. A133–A138, DOI: [10.1364/OE.18.00A133](https://doi.org/10.1364/OE.18.00A133).
- [36] LANDY N.I., SAJUYIGBE S., MOCK J.J., SMITH D.R., PADILLA W.J., *Perfect metamaterial absorber*, Physical Review Letters **100**(20), 2008, article ID 207402, DOI: [10.1103/PhysRevLett.100.207402](https://doi.org/10.1103/PhysRevLett.100.207402).
- [37] AVITZOUR Y., URZHUMOV Y.A., SHVETS G., *Wide-angle infrared absorber based on a negative-index plasmonic metamaterial*, Physical Review B **79**(4), 2009, article ID 045131, DOI: [10.1103/PhysRevB.79.045131](https://doi.org/10.1103/PhysRevB.79.045131).
- [38] HEDAYATI M.K., JAVAHERIRAHIM M., MOZOONI B., ABDELAZIZ R., TAVASSOLIZADEH A., CHAKRAVADHANULA V.S.K., ZAPOROTCHENKO V., STRUNKUS T., FAUPEL F., ELBAHRI M., *Design of a perfect black absorber at visible frequencies using plasmonic metamaterials*, Advanced Materials **23**(45), 2011, pp. 5410–5414, DOI: [10.1002/adma.201102646](https://doi.org/10.1002/adma.201102646).
- [39] ZHU P., GUO L.J., *High performance broadband absorber in the visible band by engineered dispersion and geometry of a metal-dielectric-metal stack*, Applied Physics Letters **101**(24), 2012, article ID 241116, DOI: [10.1063/1.4771994](https://doi.org/10.1063/1.4771994).
- [40] ALVES F., KEARNEY B., GRBOVIC D., LAVRIK N.V., KARUNASIRI G., *Strong terahertz absorption using SiO_2/Al based metamaterial structures*, Applied Physics Letters **100**(11), 2012, article ID 111104, DOI: [10.1063/1.3693407](https://doi.org/10.1063/1.3693407).
- [41] MO MAN-MAN, WEN QI-YE, CHEN ZHI, YANG QING-HUI, QIU DONG-HONG, LI SHENG, JING YU-LAN, ZHANG HUAI-WU, *Strong and broadband terahertz absorber using SiO_2 -based metamaterial structure*, Chinese Physics B **23**(4), 2014, article ID 047803, DOI: [10.1088/1674-1056/23/4/047803](https://doi.org/10.1088/1674-1056/23/4/047803).
- [42] YE Y.Q., JIN Y., HE S., *Omnidirectional, polarization-insensitive and broadband thin absorber in the terahertz regime*, Journal of the Optical Society of America B **27**(3), 2010, pp. 498–504, DOI: [10.1364/JOSAB.27.000498](https://doi.org/10.1364/JOSAB.27.000498).
- [43] JIA X., WANG X., YUAN C., MENG Q., ZHOU Z., *Novel dynamic tuning of broadband visible metamaterial perfect absorber using graphene*, Journal of Applied Physics **120**(3), 2016, article ID 033101, DOI: [10.1063/1.4956437](https://doi.org/10.1063/1.4956437).
- [44] ZHOU J., DONG J., WANG B., KOSCHNY T., KAFESAKI M., SOUKOULIS C.M., *Negative refractive index due to chirality*, Physical Review B **79**(12), 2009, article ID 121104(R), DOI: [10.1103/PhysRevB.79.121104](https://doi.org/10.1103/PhysRevB.79.121104).
- [45] JIA X., WANG X., *Design of a polarization-independent, wide-angle, broadband visible absorber*, Journal of Modern Optics **65**(2), 2018, pp. 129–135, DOI: [10.1080/09500340.2017.1380240](https://doi.org/10.1080/09500340.2017.1380240).
- [46] LI J., YU P., TANG C., CHENG H., LI J., CHEN S., TIAN J., *Bidirectional perfect absorber using free substrate plasmonic metasurfaces*, Advanced Optical Materials **5**(12), 2017, article ID 1700152, DOI: [10.1002/adom.201700152](https://doi.org/10.1002/adom.201700152).

Received March 6, 2018
in revised form May 3, 2018